Journal of Microwaves, Optoelectronics and Electromagnetic Applications, Vol. 22, No. 2, June 2023
DOI: http://dx.doi.org/10.1590/2179-10742023v22i2272846

A Modified Radiopropagation Multipath Model for Constant Refractivity Gradient Profiles

D. Parada[1], C. G. Rego[2], D. Guevara[3], A. Navarro[4] G. L. Ramos[5] R. Oliveira[1]
[1]*Graduate Program in Electrical Engineering - Universidade Federal de Minas Gerais - Av. Antônio Carlos 6627, Belo Horizonte, MG, Brazil, diegoandrespr@ufmg.br, roliveirabh@ufmg.br*
[2]*Departament of Electronics Engineering, Universidade Federal de Minas Gerais, Belo Horizonte, MG, CEP 31270-901, Brazil, cassio@cpdee.ufmg.br*
[3]*Departament of Electricity and Electronics, Universidad Francisco de Paula Santander, Cúcuta, Norte de Santander, CEP 540003, Colombia, dinaelgi@ufps.edu.co*
[4]*Departament of Information and Communication Technologies, Universidad ICESI, Cali, Valle del Cauca, CEP 760031, Colombia, anavarro@icesi.edu.co*
[5]*Departament of Telecommunications and Mechatronics Engineering, Federal University of São João del-Rei, Ouro Branco, MG, CEP 36415-000, Brazil, glaucio@ufsj.edu.br*

***Abstract*— This paper presents a radiopropagation algorithm based on a Ray Tracing (RT) technique that combines a modified multipath model for constant refractivity gradient profiles and the Uniform Theory of Diffraction (UTD). A novel formulation is proposed by the authors for calculation and ground-reflection analysis of ray paths depending on atmospheric refractivity. The algorithm introduced herein was evaluated in a mixed scenario and in two more realistic case studies, under conditions of constant refractivity gradient and lossy terrain profiles. Pathloss results are obtained and compared with Parabolic Equation (PE) numerical solution results at 2.0 GHz, 3.5 GHz and 5.4 GHz. In such conditions, the modified radiopropagation multipath algorithm with atmospheric refractivity introduced herein showed satisfactory results.**

***Index Terms*—**Atmospheric refractivity, multipath model, UTD, PE numerical solution, RT techniques.

I. Introduction

Latest technologies of Fifth-Generation (5G) wireless networks are aimed to the meeting of the objectives of high-speed transmission and large increase in channel capacity [1], [2]. It is awaited that 5G systems configure heterogeneous networks of overlapping cell, also composed of macrocells for wide coverage. Several sub-6 GHz frequencies are being tested for pioneering 5G services, specifically, 750 MHz, 2.5 GHz, 3.5 GHz and 5.4 GHz bands are proposed in Latin American countries to be used in 5G applications [3]. Within this framework, one of the main challenges of these technologies is to guarantee connectivity and to provide broadband services in rural and sub-urban areas. Thus, improved, quick and refined propagation models must be proposed to predict coverage and characterize the radio channel in this kind of scenarios, and at the mentioned frequency bands.

Many two-dimensional (2-D) space implementations can be found in the literature to solve radiopropagation problems, where numerical techniques such as Parabolic Equation (PE) model, Finite Difference (FD), Method of Moments (MoM), Finite Element Method (FEM) and Finite-Difference Time-Domain (FDTD) method have been successfully implemented in closed and open environments

Brazilian Microwave and Optoelectronics Society-SBMO *received 11 Mar 2023; for review 14 Mar 2023; accepted 2 May 2023*
Brazilian Society of Electromagnetism-SBMag *© 2023 SBMO/SBMag* CC BY *ISSN 2179-1074*

[4]. These numerical techniques are convenient for estimating coverage, however, bandwidth wireless communications require a suitable channel characterization. In this sense, numerical techniques are not so intuitive when it comes to temporarily characterizing the radio channel, instead optical Ray Tracing (RT) algorithms are speculated to be the most attractive in such situation [5]. Optical RT is a well-known technique used to characterize radio communication channels, and it is based on the asymptotic methods of Geometrical Optics (GO) and the Uniform Theory of Diffraction (UTD) [6], [7]. GO determines incident and reflected fields and UTD solves the edge diffraction.

The non-homogeneous behavior of atmospheric refractivity affects the radiowave propagation, such influence results in multipath fading events and interference effects, which significantly affect the long-range communications performance [8], [9]. To consider refractive properties of the atmosphere, Valtr and Pechach introduced a RT formulation for the analytical description of ray paths under a constant refractivity gradient along the height (i.e., the variation of the refractive index value only depends on the height) [10], [11]. A previous work by these same authors described an analytical RT approach for a horizontally variable refractivity height profile [12]. Nevertheless, the applicability of these models is limited to cases of line-of-sight between transmitter and receiver, and to cases where the terrain influence is not significant.

The previous works focused on solutions and results for direct ray paths considering atmospheric refractive, and up to the best knowledge of the authors, ray paths solutions associated with other propagation mechanisms have not been published. Therefore, with the objective of developing a RT technique to estimate coverage and characterize the radio channel in more realistic scenarios (considering atmospheric refractivity and terrain influence), our research proposes to complement the analytical RT approach presented in [10]–[12]. In this work, it is deduced a formulation to incorporate ground-reflection analysis, on both flat and sloping terrain. Furthermore, we employ UTD principles for the inclusion of terrain diffraction. This means that the radiopropagation algorithm, proposed in this article, predicts multipath components for the launched rays from a transmitter to a receiver point through the processing of specular reflections, diffractions, free space attenuation, and multiple combinations of those effects. In this context, the main contribution is to obtain an algorithm based on a RT technique that combines a modified multipath model with atmospheric refractivity effect and UTD.

This research assumes an academic challenge when it decides to novelly obtain a complete multipath model that considers the atmospheric refractivity effect in RT techniques from the calculation of ray paths. This implies deduction of new formulation and combination with UTD principles. The purpose is to offer a more complete solution with respect to other approaches, such as the spherical Earth model, which deform space or approximate terrain profiles. Therefore, we propose a properly deterministic approach.

A mixed scenario, which combines canonical elements, and two realistic conditions cases (Cúcuta city and Colombian Pacific Region) are used to evaluate the applicability and performance of the Modified RT algorithm proposed in this work. The Cúcuta city case combines mountainous terrain and variations in atmospheric refractivity, which are conditions typical of Andean and tropical countries. The Colombian Pacific region is a vast region of tropical rain forest, with disperse afro and indigenous communities, with a complex geography and lack of connectivity. The obtained results are confronted with the Discrete Mixed Fourier Transform (DMFT) approach of the Split Step Parabolic Equation (SSPE) numerical solution, which has been validated in previous works [13]–[15].

Brazilian Microwave and Optoelectronics Society-SBMO *received 11 Mar 2023; for review 14 Mar 2023; accepted 2 May 2023*
Brazilian Society of Electromagnetism-SBMag *© 2023 SBMO/SBMag* CC BY *ISSN 2179-1074*

This paper is organized as follows: Section II presents the formulation about ray paths considering atmospheric refractivity, Section III describes a proposed algorithm for a Modified RT technique, the case studies and results are shown in Section IV, and the conclusions are presented in Section V.

II. RAY PATHS UNDER CONSTANT REFRACTIVITY GRADIENT

Using GO assumptions, the following equation describes the ray paths depending on a refractive index n [16],

$$\frac{d}{dl}\left(n(\mathbf{r})\frac{d\mathbf{r}}{dl}\right) = \nabla n(\mathbf{r}) \tag{1}$$

where $\mathbf{r}$ represents the position vector and l is the coordinate associated with the path. We assume a 2-D propagation in Cartesian coordinates system (x is distance and z is height), a predominantly horizontal propagation ($dl \approx dx$) and also that $n(\mathbf{r})$ is a function of height, $n(\mathbf{r}) = n(z)$. Thus, Eq. (1) is rewritten as:

$$\frac{d^2z}{dx^2} = \frac{1}{n(z)}\frac{d}{dz}n(z) \tag{2}$$

where $n(z) = n_0 + \delta z$. In this expression, n_0 and δ are the surface value and the gradient of the refractive index of the medium, respectively [10]. When $n(z)$ is very close to 1 for all heights, it is possible to represent Eq. (2) as:

$$\frac{d^2z}{dx^2} = \frac{d}{dz}n(z) = \frac{d}{dz}(n_0 + \delta z) = \delta. \tag{3}$$

The solution to Eq. (3) is given by [15]:

$$z = \frac{\delta x^2}{2} + x\tan\alpha + Z_T. \tag{4}$$

Eq. (4) denotes the dependency of the ray path on the x coordinate, on the transmitter height Z_T and on the launch angle of the ray α, as shown in Fig. 1.

A. Direct ray analysis

Knowing the location of a receiver point, the launch angle of the direct ray can be obtained from:

$$\alpha = \arctan\left(\frac{\Delta Z_R + Z_R - Z_T}{R}\right), \tag{5}$$

where $\Delta Z_R = \delta R^2/2$, Z_R is the receiver height, and R is the distance from the transmitter to the receiver point (see Fig. 1).

B. Incident and reflected rays on flat terrain

The deduced formulation for ground-reflection analysis has been partially presented by the authors of this work in international conference papers. This approach is proposed when the location of a receiver point is known on flat terrain. Therefore, we deduce a formulation to calculate the location of a reflection point. Fig. 2 shows the incident and reflected ray paths and it can also be seen that incident ray and reflected ray at $x = X$ make an angle α_1 and α_2 with the parallel to the earth plane, respectively. From Snell's law

$$\alpha_1 = \alpha_2, \tag{6}$$

Brazilian Microwave and Optoelectronics Society-SBMO *received 11 Mar 2023; for review 14 Mar 2023; accepted 2 May 2023*
Brazilian Society of Electromagnetism-SBMag *© 2023 SBMO/SBMag* CC BY *ISSN 2179-1074*

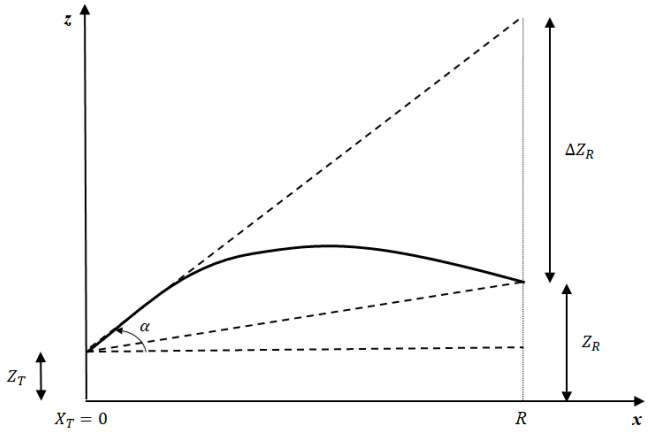

Fig. 1. Direct ray path.

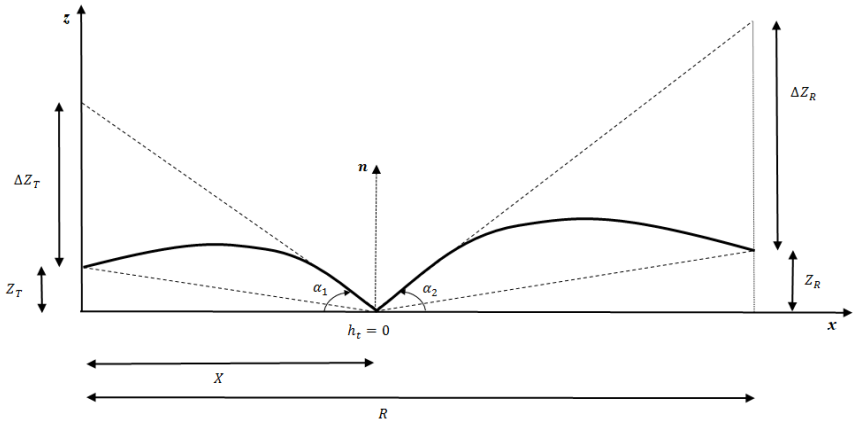

Fig. 2. Incident and reflected ray paths on flat terrain.

and using the reciprocity theorem (in order to analyze a given antenna in transmitting or receiving mode), the variables exhibited in Fig. 2 and Eq. (5), we can write α_1 and α_2 as follows:

$$\alpha_1 = \arctan\left(-\frac{\delta X}{2} + \frac{Z_T}{X}\right), \tag{7}$$

$$\alpha_2 = \arctan\left(-\frac{\delta(R-X)}{2} + \frac{Z_R}{R-X}\right). \tag{8}$$

Substituting the expressions (7) and (8) into Eq. (6), we obtain a cubic equation [15]:

$$X^3(\delta) - X^2\left(\frac{3\delta R}{2}\right) + X\left(\frac{\delta R^2}{2} - Z_R - Z_T\right) + RZ_T \;=\; 0. \tag{9}$$

The unknown X is the distance from the transmitter to the reflection point, and its solution is given by a real root $X = x_1$, minimum value and $x_1 > 0$. So the reflection point is at the coordinate $(X, 0)$, as can be seen in Fig. 2.

C. Analysis of incident and reflected rays over sloping terrain

In the same way as in flat terrain case, our purpose is to offer a formulation that calculates a reflection point over sloping terrain. The terrain is modeled by $z = mx$, where m is the slope of the terrain. According to Fig. 3, the following mathematical relationships are deduced:

© 2023 SBMO/SBMag CC BY
ISSN 2179-1074

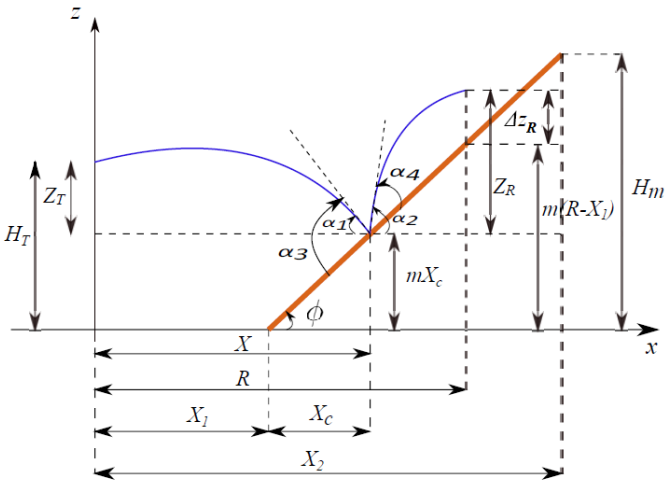

Fig. 3. Incident and reflected ray paths over a sloping terrain.

$$\tan\phi = \frac{H_m}{X_2 - X_1} = m, \tag{10}$$

$$X = X_1 + X_c, \tag{11}$$

$$Z_T = H_T + mX_1 - mX, \tag{12}$$

$$Z_R = \Delta z_R + mR - mX, \tag{13}$$

where, as depicted in Fig. 3, Δz_R is the height of a receiver point over terrain, ϕ corresponds to the angle associated with the slope of the terrain, H_T refers to the transmitter height for this situation, H_m is the maximum height of the wedge, X_1 represents the distance from the transmitter to the initial location of the sloping terrain, X_C is the distance from the initial location of sloping terrain to the reflection point and X_2 indicates the distance from the transmitter to the final location of the sloping terrain.

Based on Fig. 3 and Snell's law, it is known that $\alpha_3 = \alpha_4$, which can be rewritten as:

$$\alpha_1 + \phi = \alpha_2 - \phi, \tag{14}$$

where α_1 and α_2 correspond to the incident and reflected angles, respectively, with respect to a horizontal reference line (Fig. 3). Similarly, α_3 and α_4 refer to the incident angle and reflected angle with respect to sloping terrain. Manipulating mathematically, we have:

$$\tan(\alpha_1 + \phi) = \tan(\alpha_2 - \phi). \tag{15}$$

Therefore, we use some trigonometric properties to reach at the following expression:

$$\tan\alpha_1 - \tan\alpha_2 + 2\tan\phi + 2\tan\alpha_1\tan\alpha_2\tan\phi + \tan^2\phi(\tan\alpha_2 - \tan\alpha_1) = 0. \tag{16}$$

Now, substituting the expressions (7), (8), (10), (11), (12) and (13) into Eq. (16), it is possible to obtain a fourth degree equation:

$$AX^4 + BX^3 + CX^2 + DX + E = 0, \tag{17}$$

© 2023 SBMO/SBMag CC BY

where the coefficients are defined in terms of δ and the variables exhibited in Fig. 3, as shown from expression (18) to (22) [17]:

$$A = \delta^2 m, \tag{18}$$

$$B = -2\delta^2 mR + 2\delta(1+m^2), \tag{19}$$

$$C = \delta^2 mR^2 - \delta(3R + 2m\Delta z_R + 2mH_T + 3m^2 R + 2m^2 X_1), \tag{20}$$

$$D = \delta(R^2 - R^2 m^2 + 4mRH_T + 4m^2 RX_1 - 2m^3 R^2) - 2(H_T + mX_1 + \Delta z_R + m^2 H_T + m^2 \Delta z_R + m^3 X_1), \tag{21}$$

$$E = -2\delta(mR^2 H_T + m^2 R^2 X_1) + 2(RH_T + RmX_1 + 2mH_T \Delta z_R + m^2 RH_T + 2m^2 \Delta z_R X_1 + m^3 RX_1). \tag{22}$$

In Eq. (17) the solution is given by a real root $X = x_1$, maximum value and $x_1 > 0$. Therefore, the reflection point is at the coordinate $(\ X, m(X - X_1)\ )$.

The UTD approach used in this multipath algorithm proposal is based on the Lubbers coefficients. More details about the used UTD formulation are presented in Section III-C.

III. Proposed Algorithm for a Modified Radiopropagation Multipath Model

The algorithm is shown in Fig. 4 as a flowchart. The direct ray, reflection and diffraction analysis, are implemented by three blocks (see Fig. 4) which are executed in parallel. To run those three blocks it is necessary to know the following input parameters: electromagnetic properties, refractivity gradient of the medium, and locations of the transmitter and receiver.

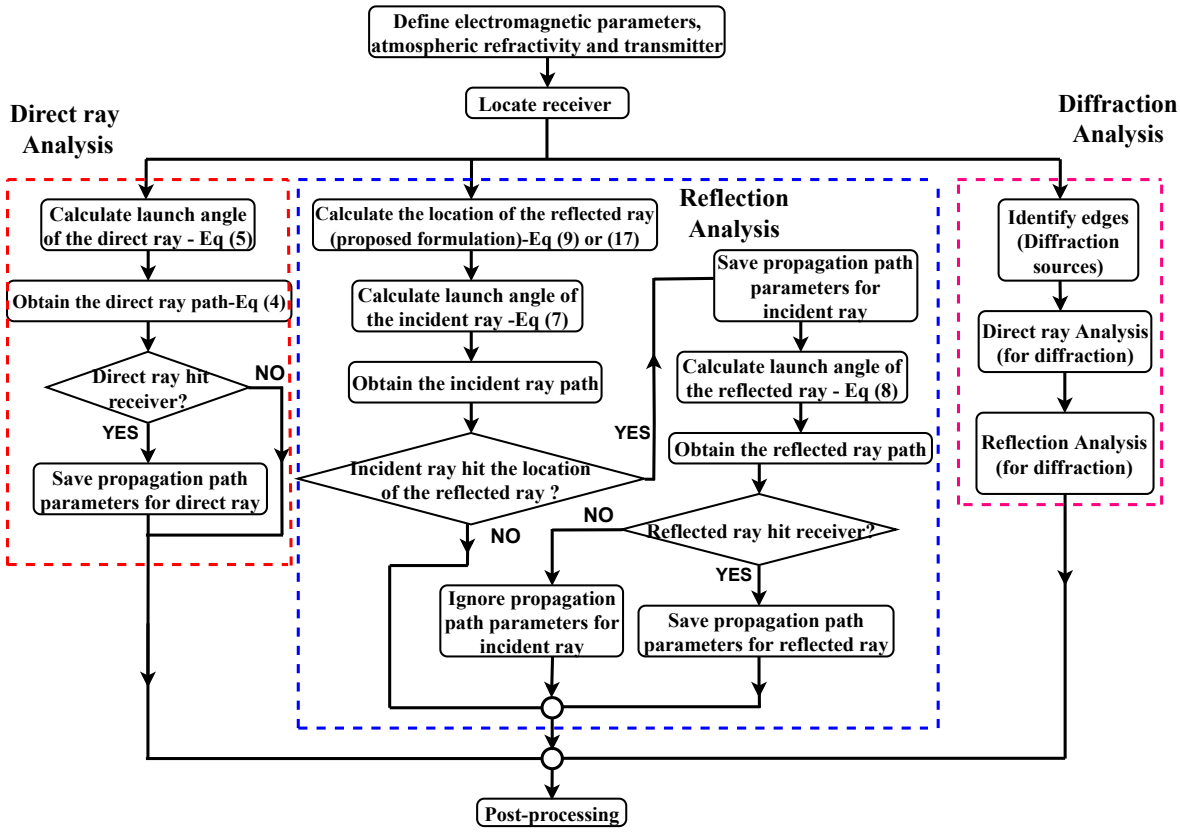

Fig. 4. Flowchart for a modified multipath model based on RT techniques.

© 2023 SBMO/SBMag CC BY

A. Direct ray analysis

Knowing the input parameters, the launch angle of the direct ray is calculated according to Eq. (5), then the direct ray path is obtained from Eq. (4). In the next step, it is investigated if a direct ray hits the receiver. If the algorithm identifies that the receiver is reached, it proceeds to save the path parameters, and then, continues to post-processing. Otherwise, the algorithm ignores the direct ray path and continues to post-processing.

Two situations can occur so that a ray path does not hit on a receiver point. The first situation is that the algorithm identifies that there is an obstacle that interrupts the ray path. The second one is that due to the curvature of the ray path, it cannot reach the receiver. These above criteria are applied to direct, incident and reflected ray paths.

B. Reflection analysis

The location of the reflection point is calculated by using the formulation proposed herein, Eq. (9) or Eq. (17) is used depending on the situation, either flat or sloping terrain. Once known the location where the ground-reflection occurs, it is possible to calculate the launch angle of the incident ray from Eq. (7), then the incident ray path is obtained. In the next step, it is investigated if the obtained incident ray path hits the location of the point reflection. If the algorithm identifies that the reflection point is reached, it proceeds to save the path parameters. Otherwise, the algorithm ignores the obtained incident ray path and continues to post-processing.

If the incident ray path hits the reflection point, it is possible to calculate the launch angle of the reflected ray from Eq. (8), then, the reflected ray path is obtained as indicated by Fig. 4. In the next step, it is learned if the reflected ray path hits the location of the receiver point. If the algorithm identifies that the receiver point is reached, it proceeds to save the path parameters, and then, continues to post processing. Otherwise, the algorithm ignores the obtained reflected ray path and the path parameters for incident ray, consequently, continues to post-processing.

C. Diffraction analysis

The algorithm has the ability to identify edges that generate diffraction. An analysis of direct, incident and reflected rays associated with the diffraction phenomenon is carried out.

The UTD formulation considers the 2-D problem of diffraction by a semi-infinite wedge with straight edges. The geometry and wedge diffraction variables involved in the formulation can be seen in [18]. The distances between the source and the wedge, and between the wedge and the observation point, are calculated with the optical length equation [11]. The general UTD solution for the electric field at the observation point is:

$$E_d(O) = E_i(W) \cdot \overline{D} A(s_d) e^{-jks_d} \tag{23}$$

where, $E_i(W)$ is the incident electric field at the edge of the wedge, $A(s_d)$ is the amplitude factor, s_d is the distance between wedge and observer, and $\overline{D}$ is the dyadic diffraction coefficient. Assuming the classical notation of [19], the dyadic soft and hard is given as follows:

$$\overline{D}^{s,h} = G_0^{s,h}\left[D_2 + R_0^{s,h}(\alpha_0)D_4\right] + G_n^{s,h}\left[D_1 + R_n^{s,h}(\alpha_n)D_3\right] \tag{24}$$

where D_i, for $i = 1, \ldots, 4$, are the UTD diffraction coefficients, G_0 and G_n, are grazing incidence factor, R_0 and R_n are Fresnel reflection coefficients, for the analyzed faces of the wedge. The UTD

received 11 Mar 2023; for review 14 Mar 2023; accepted 2 May 2023
© 2023 SBMO/SBMag CC BY
ISSN 2179-1074

formulation is based on the Fresnel reflection coefficients, specifically, the Lubbers Coefficients [20] defining the incidence and reflection angles of the incident and diffracted rays.

D. Post-processing

Everytime that a ray hits a receiver point, the following path parameters are computed and saved by our algorithm: $\tau_i(t)$: time delay of arrival (TDA) of path, $\overline{T}_i(t)$: polarimetric transmission matrix of path, $\Omega_{T,i}(t)$: direction of departure (DoD) of path and $\Omega_{R,i}(t)$: direction of arrival (DoA) of path. In order to calculate the total EM field at each receiver point, a coherent sum is computed, taking into account the individual contribution of each multipath component.

In the case studies carried out in Section IV, the following propagation mechanisms are processed by the algorithm: a direct ray path, an incident-reflected ray path, diffraction ray paths and diffraction-reflection combinations arriving at the receiver point, accumulating in maximum two consecutive propagation mechanisms (see Fig. 8, in Section IV-B).

IV. Case Studies and Results

The first case study consists of a mixed scenario to validate our proposal on a test that combines several canonical elements. Then, two realistic cases studies are carried out to verify the applicability of our radiopropagation modeling in environments that combine lossy terrain profiles and refractivity variation conditions. The frequencies used in the simulations correspond to the bands projected to offer 5G services. In all case studies, comparisons are made between a modified multipath algorithm and the DMFT-SSPE numerical solution for pathloss results. In addition, to demonstrate the ability to characterize the radio channel in realistic cases, Power Delay Profiles (PDP) are obtained through the proposed multipath algorithm.

A. Mixed scenario

The environment is a mixed scenario, with a total extension of 40 km. The terrain profile is a lossy wedge of 80 m height and centered at 20 km, and whose initial and final positions are located at 12 km and 28 km, respectively. In this case study, the ground region is characterized as a standard ground surface (ϵ_r=15 and $\sigma = 0.012$ S/m) and a saltwater region (ϵ_r=81 and $\sigma = 2$ S/m) is placed behind the wedge, from 28 km to 32 km. The refractivity variation is modeled as: $N(z) = 304 - 100z$, a linearly decreasing refractivity altitude profile, which corresponds to a surface duct [21]. In this work, we use a gradient of modified refractive index $dm/dz = dn/dz + 1.57 \times 10^{-7}$ [12]. The transmitter is located at 100 m height, the simulation uses a frequency of 5.4 GHz and vertical polarization.

The source is modeled as a Gaussian antenna beam pattern. In most 2-D long-range radiopropagation models, this type of source modeling is chosen because it can adjust beamwidth and beam tilt and provide an approximate representation for paraboloid dish antennas [22].

In order to calculate the pathloss horizontal profile using the Modified RT algorithm, we define the horizontal step size ($\Delta x = 10$ m) and receiver points located at 10 m height along the terrain. Likewise, the vertical step size ($\Delta z = 0.16$ m) is used to calculate the pathloss vertical profile at $x = 32$ km.

Fig. 5 shows the scenario scheme and depicts the conformation of ray paths to calculate the pathloss horizontal using the Modified RT algorithm. In Fig. 6 the 2-D received power distribution achieved with DMF-SSPE is shown. In this graph, the very low levels of received power that are perceived at the

Brazilian Microwave and Optoelectronics Society-SBMO *received 11 Mar 2023; for review 14 Mar 2023; accepted 2 May 2023*
Brazilian Society of Electromagnetism-SBMag *© 2023 SBMO/SBMag* CC BY *ISSN 2179-1074*

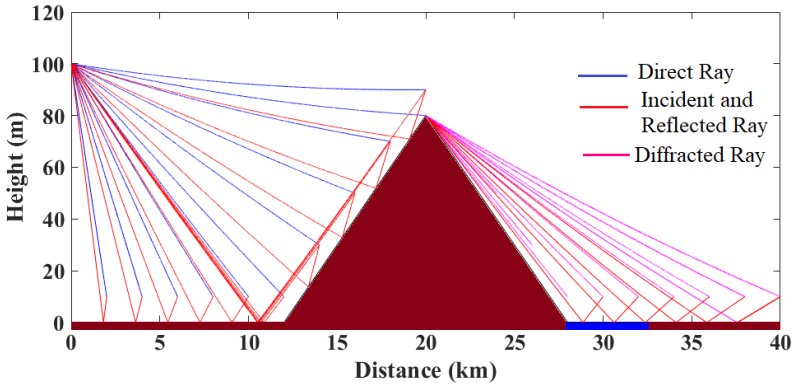

Fig. 5. Scenario scheme and ray paths to calculate a pathloss horizontal profile using $dN/dz = -100$ N/km.

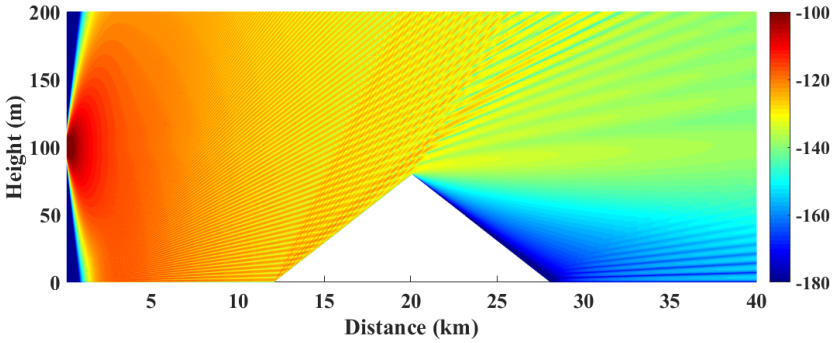

Fig. 6. Received Power (dBW) vs. distance-height obtained with DMFT-SSPE for mixed scenario at 5.4 GHz.

closest distances to the transmitter are not expected, since it does not correspond to a natural behavior of the phenomenon. However, this response is due to the shape of the directional Gaussian antenna pattern used in the simulations. To estimate a pathloss horizontal profile, a correct range of receiver points is chosen, from 1.5 km to 40 km. In Fig. 7 the comparison between the proposed Modified RT and DMFT-SSPE numerical algorithm is presented. The horizontal and vertical profiles for pathloss results are illustrated, respectively, in Figs. 7(a) and 7(b).

The statistics are summarized in Table I. It is possible to observe that a good agreement is obtained in statistic comparison between our proposal of a Modified RT and DMFT-SSPE results.

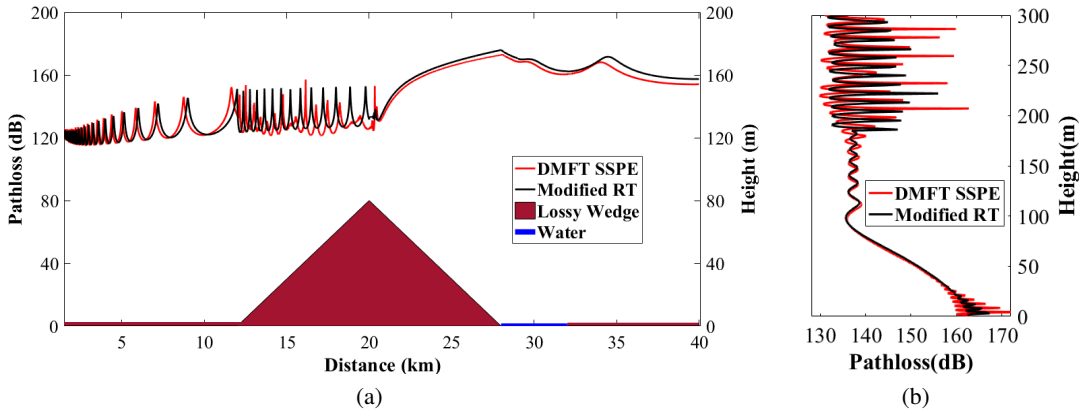

Fig. 7. Pathloss results: (a) Horizontal Profile at 10 m height and (b) Vertical profile at x =32 km.

© 2023 SBMO/SBMag CC BY

TABLE I. STATISTIC COMPARISON FOR PATHLOSS RESULTS IN MIXED SCENARIO CASE

Pathloss Profile	Mean Absolute Difference (dB)	Standard Deviation (dB)
Horizontal	4.45	6.17
Vertical	2.90	4.92

B. Cúcuta city case

This first realistic scenario is located in Cúcuta city (Colombia). It consists of a terrain profile with an approximate extension of 15 km, the surface is characterized as a standard ground and the refractivity variation is modeled as: $N(z) = 305.66 - 60z$, according to Recommendation ITU-R P.453-14 for the environmental conditions of the mentioned city. The terrain profile information is collected using the NASA Shuttle Radar Topography Mission (SRTM) Version 3.0 dataset.

The transmitter is located at 100 m height and the simulation uses a frequency of 2.0 GHz and vertical polarization. To calculate the pathloss horizontal profile, both techniques use a horizontal step size ($\Delta x = 50$ m) and the receiver points are located at 10 m height along the terrain.

Fig. 8 shows the conformation of ray paths at $x = 1000$ m and 10 m height to calculate Pathloss and the PDP at this receiver point through the Modified RT algorithm. In Fig. 9 the PDP is depicted, in this way, the ability of the proposed algorithm to characterize the radio channel is demonstrated.

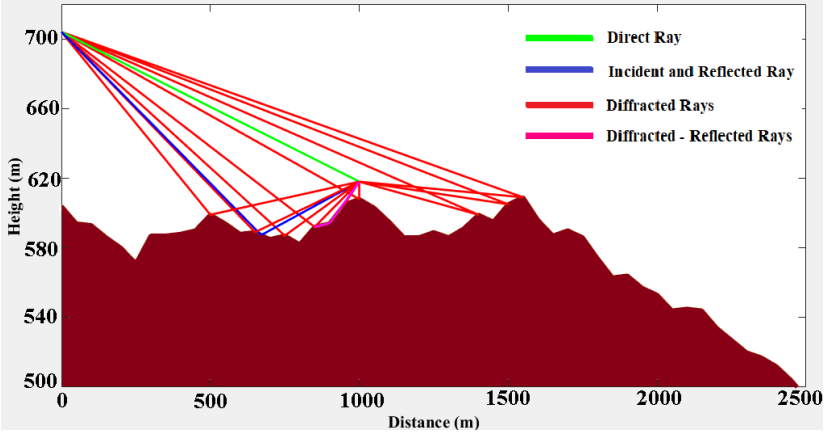

Fig. 8. Ray paths to calculate Pathloss results and PDP by using a Modified RT algorithm.

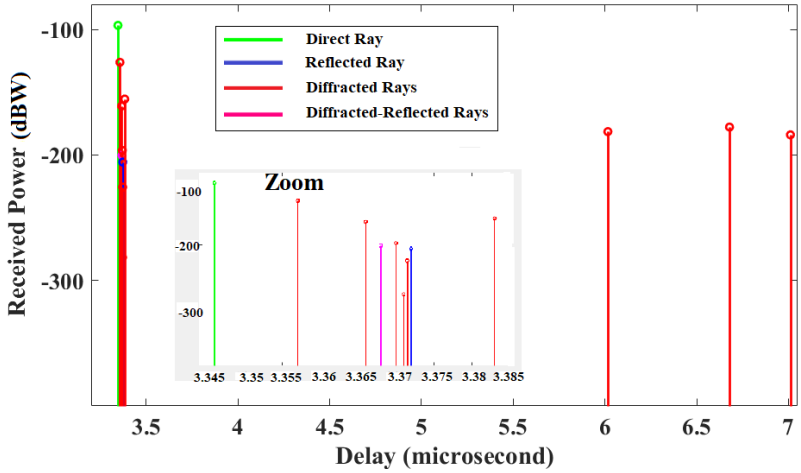

Fig. 9. Power Delay Profile at $x = 1000$ m and 10 m height.

© 2023 SBMO/SBMag CC BY

It is possible to obtain a 2-D received power distribution with DMFT-SSPE, since this numerical approach allows to discretize and calculate the EM field solution of the entire analyzed scenario. Hence, we generate Fig. 10 using a DMFT-SSPE algorithm, which is implemented computationally by the authors of this work. In Fig. 10, it can be seen that at shorter distances there are Non-Line-of-Sight (NLOS) regions, due to the particularities of the terrain profile of the analyzed scenario, and taking into account that the height of the receiver points is 10 m. Furthermore, it is also possible to note that at longer distances there are line-of-sight (LOS) regions, and consequently, this propagation mechanism implies a greater contribution to the final value of received signal intensity at those receiver points. The previously described can be observed in the results of the pathloss curves obtained along the terrain profile (see Fig. 11).

In this realistic case, we also obtain results from a RT technique that does not consider atmospheric effects, denominated Non-Modified RT. The purpose is to observe if the inclusion of atmospheric refractivity in the RT technique leads to promising results, when comparing the results obtained with respect to reliable and consolidated techniques, such as the DMFT-SSPE numerical approach. Fig. 11(a) illustrates the comparison of the pathloss horizontal profile results obtained with the Non-Modified RT and DMFT-SSPE tecniques. Similarly, Fig. 11(b) shows the pathloss curves results obtained with the proposed Modified RT algorithm and DMFT-SSPE solution.

In Fig. 11 it can be observed that in some positions no results are obtained, this happens because our RT algorithms use basic combinations of propagation mechanisms and therefore the ray paths do not hit on certain observation points. The proposed alternative is the combination of many more propagation mechanisms, however, this approach generates a high computational cost. The simulations show that the non-hit points of the Non-Modified and the Modified RT are different, which is explained by the slightly different path that the inclusion of atmospheric refractivity effect produces.

Table II summarizes the statistics. It can be perceived that a Modified RT algorithm shows a encouraging result in statistical comparison. However, in order to consolidate a conclusion about the results obtained with the proposed algorithm, it is necessary to analyze its performance and behavior in another scenario and at a different frequency band.

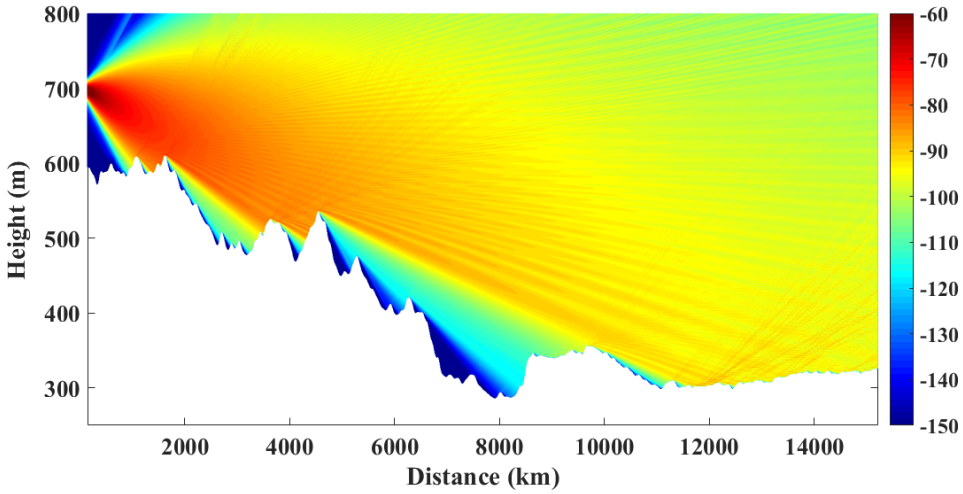

Fig. 10. Received Power (dBW) vs. distance-height obtained with DMFT SSPE for Cúcuta city case at 2.0 GHz.

© 2023 SBMO/SBMag CC BY

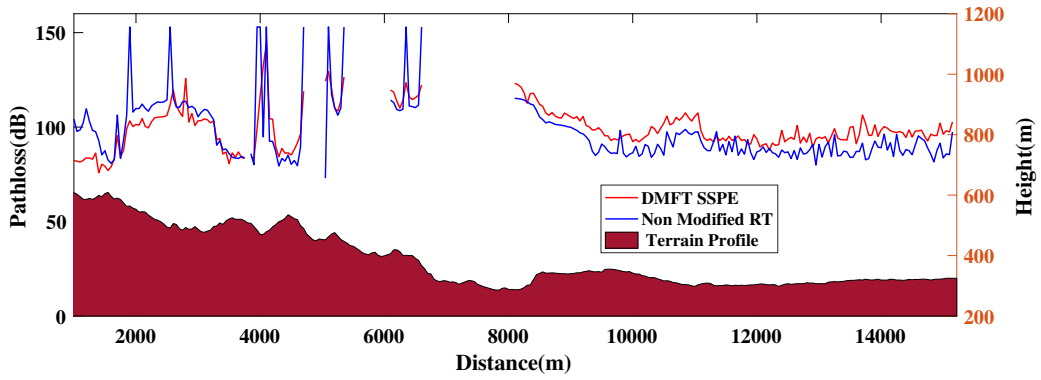

(a)

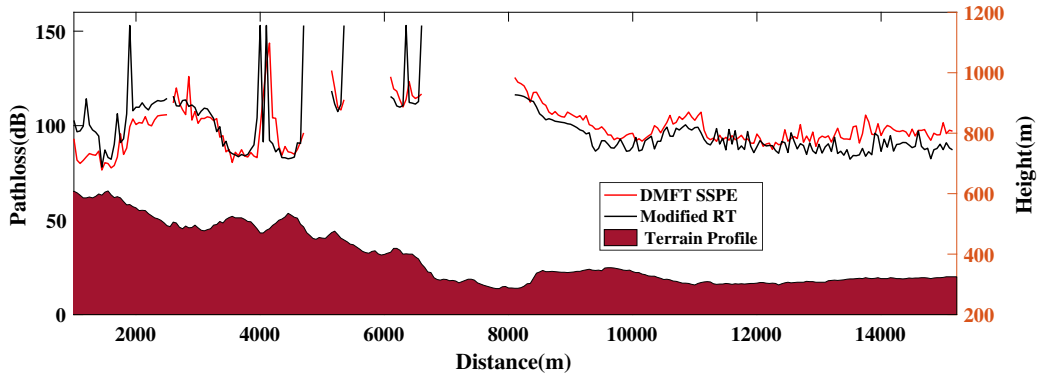

(b)

Fig. 11. Pathloss Horizontal Profile results for Cúcuta city case: (a) Non-Modified RT versus DMFT-SSPE and (b) Modified RT versus DMFT-SSPE.

TABLE II. STATISTIC COMPARISON FOR PATHLOSS RESULTS IN CÚCUTA CITY CASE

RT Technique	Mean Absolute Difference (dB)	Standard Deviation (dB)
Non Modified	8.55	11.75
Modified	7.84	11.57

C. Pacific region case

This second realistic scenario is located in the Colombian Pacific Region, which is a tropical rain forest region with dispersed population, adverse geographical conditions and lack of connectivity. It consists of a rural long-range terrain profile with an approximate extension of 21 km, the surface is characterized as a damp ground ($\epsilon_r = 27$ and $\sigma = 0.02S/m$) and the refractivity variation is modeled as: $N(z) = 378 - 60z$. The transmitter is located at 25 m height, the simulation uses a frequency of 3.5 GHz and vertical polarization. In order to calculate the pathloss horizontal profile, the radiopropagation techniques use a horizontal step size (Δx = 10 m) and the receiver points are located at 30 m height along the terrain.

Fig. 12 shows the conformation of ray paths at the final position of the radio link. In this case, the direct ray path and four diffracted ray paths, produced by the terrain influence, are configured. Consequently, the PDP at this receiver point can be generated and is depicted in Fig. 13.

In the same way as in Cúcuta city case, in this case study we compare the Non-Modified RT and Modified RT results with respect to DMFT-SSPE. In Fig. 14, the pathloss curves along the terrain for

© 2023 SBMO/SBMag CC BY
ISSN 2179-1074

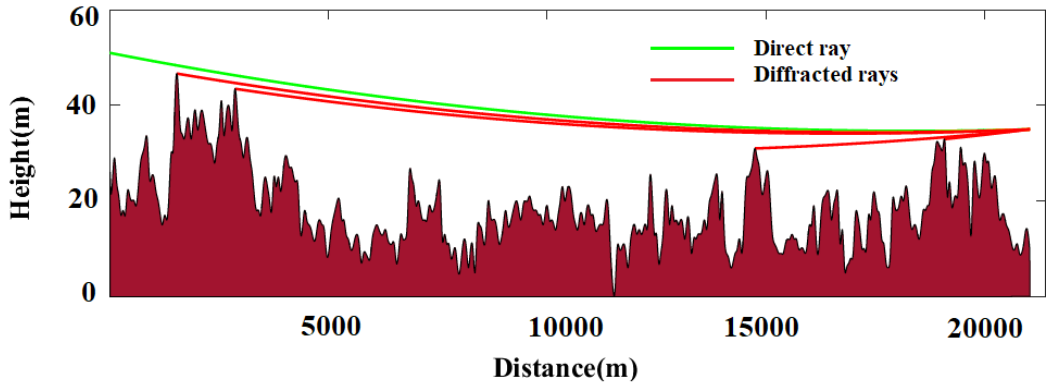

Fig. 12. Ray paths conformation at the final position of the radio link for Colombian Pacific region case.

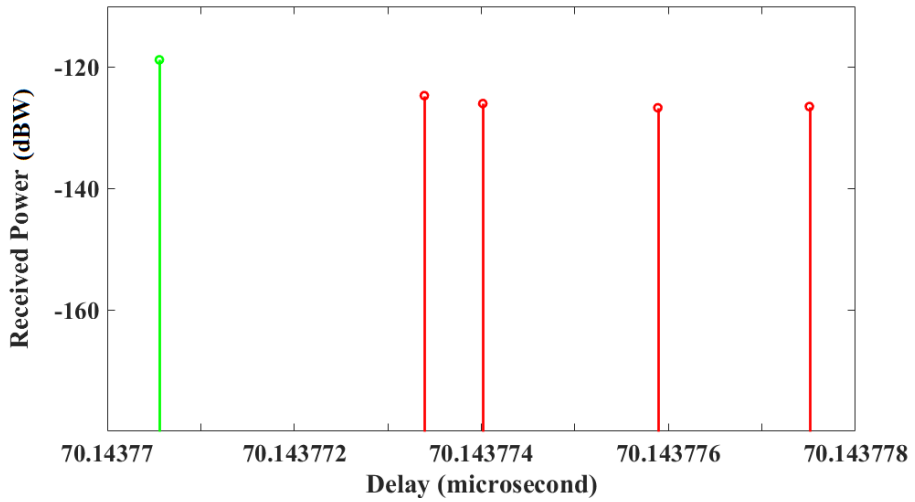

Fig. 13. Power Delay Profile at the final position of the radio link for Colombian Pacific region case.

both situations are illustrated, Figs. 14(a) and 14(b), respectively. It can be noted that unlike the first realistic case, in this environment a complete pathloss curve is obtained along the terrain, this is mainly due to the choice of higher receiver points. This means that for all the observation points considered over the Pacific region terrain profile, the proposed multipath approach achieves a combination of ray paths that hit a known receiver point.

Table III displays the statistics. Similarly to the realistic case above, it can be observed that a Modified RT algorithm shows a slightly better result in the statistical comparison.

The results obtained in both realistic cases allow to conclude that the proposal of atmospheric refractivity inclusion into a multipath approach, based on RT solutions, is a promising propagation model to be applied in this kind of environments. Additionally, the capacity of the proposed algorithm to estimate coverage and characterize radio channels at sub-6 GHz frequency bands (projected for 5G systems operation) is also demonstrated.

TABLE III. STATISTIC COMPARISON FOR PATHLOSS RESULTS IN PACIFIC REGION CASE

RT Technique	Mean Absolute Difference (dB)	Standard Deviation (dB)
Non Modified	5.05	6.04
Modified	4.88	5.89

© 2023 SBMO/SBMag CC BY
ISSN 2179-1074

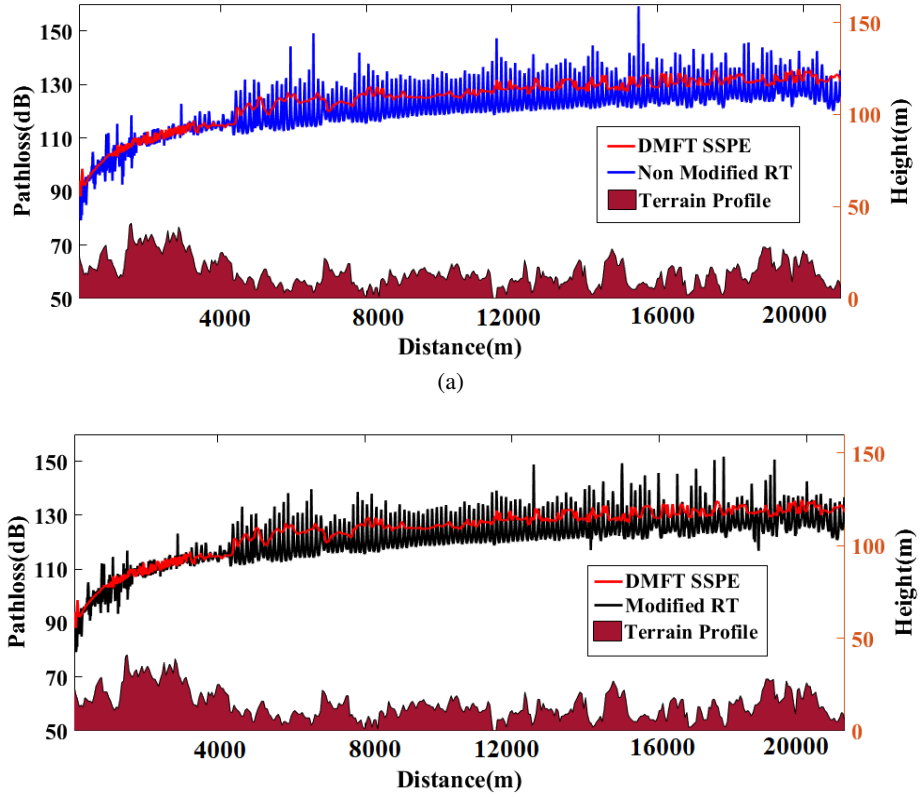

Fig. 14. Pathloss Horizontal Profile results for Pacific region case: (a) Non-Modified RT versus DMFT-SSPE and (b) Modified RT versus DMFT-SSPE.

V. Conclusions

The algorithm proposed in this work incorporates constant refractivity gradient profiles into RT technique, and therefore, a modified radiopropagation multipath algorithm is presented. In this approach, a novel formulation is deduced in order to obtain ground-reflection ray paths. Based on the obtained results, we show that the proposed modified multipath model includes favorably the atmospheric refractivity effect into RT approach. Thus, the proposed solution is a promising radiopropagation model to estimate coverage and characterize the radio channel in rural and sub-urban scenarios with more realistic conditions. The applicability of the Modified RT technique to study propagation problems at sub-6 GHz frequency bands for 5G systems was shown in this work. Finally, the Modified RT algorithm also is promising for wide coverage analysis in three-dimensional scenarios, which are more complex and where many more multipath components are configured.

Acknowledgment

This work was partially supported by CNPq project number 311521/2020-7 and CAPES.

References

[1] T. S. Rappaport, Y. Xing, G. R. MacCartney, A. F. Molisch, E. Mellios, and J. Zhang, "Overview of millimeter wave communications for fifth-generation (5G) wireless networks — With a focus on propagation models," *IEEE Transactions on Antennas and Propagation*, vol. 65, no. 12, pp. 6213–6230, 2017.

 © 2023 SBMO/SBMag CC BY *ISSN 2179-1074*

[2] A. Navarro, D. Guevara, D. Escalante, W. Cruz, J. Gómez, N. Cardona, and J. Gimenez, "Delay spread in mmwave bands for indoor using game engines 3D ray based tools," in *2016 10th European Conference on Antennas and Propagation (EuCAP)*, pp. 1–5, 2016.

[3] N. R. Leonor, S. Faria, G. Ramos, P. V. G. Castellanos, C. Rodríguez, L. da Silva Mello, and R. F. S. Caldeirinha, "Site-specific radio propagation model for macrocell coverage at sub-6 GHz frequencies," *IEEE Transactions on Antennas and Propagation*, vol. 70, no. 10, pp. 9706–9715, 2022.

[4] G. Apaydin and L. Sevgi, *Radio Wave Propagation and Parabolic Equation Modeling*. John Wiley & Sons, 2017.

[5] A. Navarro, D. Guevara, and J. Gómez, "A proposal to improve ray launching techniques," *IEEE Antennas and Wireless Propagation Letters*, vol. 18, no. 1, pp. 143–146, 2019.

[6] I. Wald, W. R. Mark, J. Günther, S. Boulos, T. Ize, W. Hunt, S. G. Parker, and P. Shirley, "State of the art in ray tracing animated scenes," in *Computer graphics forum*, vol. 28, no. 6, pp. 1691–1722, 2009.

[7] P. Y. Ufimtsev, *Fundamentals of the Physical Theory of Diffraction*. John Wiley & Sons, 2014.

[8] A. Karimian, C. Yardim, P. Gerstoft, W. S. Hodgkiss, and A. E. Barrios, "Refractivity estimation from sea clutter: An invited review," *Radio science*, vol. 46, no. 06, pp. 1–16, 2011.

[9] S. Wang, T. H. Lim, Y. J. Chong, J. Ko, Y. B. Park, and H. Choo, "Estimation of abnormal wave propagation by a novel duct map based on the average normalized path loss," *Microwave and Optical Technology Letters*, vol. 62, no. 4, pp. 1662–1670, 2020.

[10] P. Valtr and P. Pechac, "Tropospheric refraction modeling using ray-tracing and parabolic equation," *Radioengineering*, vol. 14, no. 4, pp. 98–104, 2005.

[11] ——, "Analytic tropospheric ray-tracing model for constant refractivity gradient profiles," in *2006 First European Conference on Antennas and Propagation*, pp. 1–4, 2006.

[12] ——, "The influence of horizontally variable refractive index height profile on radio horizon range," *IEEE Antennas and Wireless Propagation Letters*, vol. 4, pp. 489–491, 2005.

[13] P. Zhang, L. Bai, Z. Wu, and L. Guo, "Applying the parabolic equation to tropospheric groundwave propagation: A review of recent achievements and significant milestones." *IEEE Antennas and Propagation Magazine*, vol. 58, no. 3, pp. 31–44, 2016.

[14] O. Ozgun, G. Apaydin, M. Kuzuoglu, and L. Sevgi, "PETOOL: MATLAB-based one-way and two-way split-step parabolic equation tool for radiowave propagation over variable terrain," *Computer Physics Communications*, vol. 182, no. 12, pp. 2638–2654, 2011.

[15] A. Navarro, D. Parada, D. Guevara, C. G. Rego, and R. A. Badillo, "Modified two-ray model with UTD and atmospheric effects," in *2020 14th European Conference on Antennas and Propagation (EuCAP)*, pp. 1–5, 2020.

[16] M. Levy, *Parabolic Equation Methods for Electromagnetic Wave Propagation*. IET, 2000, no. 45.

[17] A. Navarro, D. Parada, D. Guevara, C. G. Rego, R. Oliveira, R. Velásquez, and L. Gomezjurado, "A modified two-ray model with UTD and atmospheric effects: Analysis of reflected ray Over sloping terrain," in *2021 15th European Conference on Antennas and Propagation (EuCAP)*, pp. 1–4, 2021.

[18] D. Tami, C. G. Rego, D. Guevara, A. Navarro, F. J. Moreira, J. Giménez, and H. G. Triana, "Analysis of heuristic uniform theory of diffraction coefficients for electromagnetic scattering prediction," *International Journal of Antennas and Propagation*, vol. 2018, pp. 1–11, 2018.

[19] R. G. Kouyoumjian and P. H. Pathak, "A uniform geometrical theory of diffraction for an edge in a perfectly conducting surface," *Proceedings of the IEEE*, vol. 62, no. 11, pp. 1448–1461, 1974.

[20] R. Luebbers, "A heuristic UTD slope diffraction coefficient for rough lossy wedges," *IEEE Transactions on Antennas and Propagation*, vol. 37, no. 2, pp. 206–211, 1989.

[21] F. Akleman and L. Sevgi, "A novel finite-difference time-domain wave propagator," *IEEE Transactions on Antennas and Propagation*, vol. 48, no. 5, pp. 839–841, 2000.

[22] P. Zhang, L. Bai, Z. Wu, and L. Guo, "Applying the parabolic equation to tropospheric groundwave propagation: A review of recent achievements and significant milestones," *IEEE Antennas and Propagation Magazine*, vol. 58, no. 3, pp. 31–44, 2016.

Brazilian Microwave and Optoelectronics Society-SBMO *received 11 Mar 2023; for review 14 Mar 2023; accepted 2 May 2023*
Brazilian Society of Electromagnetism-SBMag *© 2023 SBMO/SBMag* CC BY *ISSN 2179-1074*